



**HAL**  
open science

## Cyclic (Alkyl)(Amino)Carbene (CAAC) Gold(I) Complexes as Chemotherapeutic Agents

Maria T Proetto, Kelsey Alexander, Mohand Melaimi, Guy Bertrand, Nathan  
C Gianneschi

► **To cite this version:**

Maria T Proetto, Kelsey Alexander, Mohand Melaimi, Guy Bertrand, Nathan C Gianneschi. Cyclic (Alkyl)(Amino)Carbene (CAAC) Gold(I) Complexes as Chemotherapeutic Agents. Chemistry - A European Journal, In press, 10.1002/chem.202004317 . hal-03070796

**HAL Id: hal-03070796**

**<https://hal.science/hal-03070796>**

Submitted on 16 Dec 2020

**HAL** is a multi-disciplinary open access archive for the deposit and dissemination of scientific research documents, whether they are published or not. The documents may come from teaching and research institutions in France or abroad, or from public or private research centers.

L'archive ouverte pluridisciplinaire **HAL**, est destinée au dépôt et à la diffusion de documents scientifiques de niveau recherche, publiés ou non, émanant des établissements d'enseignement et de recherche français ou étrangers, des laboratoires publics ou privés.

# Cyclic (Alkyl)(Amino)Carbene (CAAC) Gold(I) Complexes as Chemotherapeutic Agents.

Maria T. Proetto,<sup>[a,b]</sup> Kelsey Alexander,<sup>[a]</sup> Mohand Melaimi,<sup>[c]\*</sup> Guy Bertrand,<sup>[c]\*</sup> and Nathan C. Gianneschi<sup>[a,b]\*</sup>

Dedication ((optional))

- [a] Dr. M. T. Proetto, K. Alexander, Pr. N. Gianneschi  
Department of Chemistry and Biochemistry, University of California San Diego, 9500 Gilman Drive, La Jolla, CA 92093, USA.  
E-mail: nathan.gianneschi@northwestern.edu
- [b] [a] Dr. M. T. Proetto, Pr. N. Gianneschi  
Department of Chemistry, Department of Materials Science & Engineering, Department of Biomedical Engineering, and Department of Pharmacology.  
International Institute for Nanotechnology, Simpson Querrey Institute, Chemistry of Life Processes Institute and Lurie Cancer Center, Northwestern  
University, Evanston, IL 60208, USA.
- [c] Dr. M. Melaimi, Pr. G. Bertrand  
UCSD-CNRS Joint Research Laboratory (UMI 3555), Department of Chemistry and Biochemistry, University of California, San Diego, La Jolla, CA 92093-  
0358, USA  
E-mail: mmelaimi@ucsd.edu; gbertrand@ucsd.edu

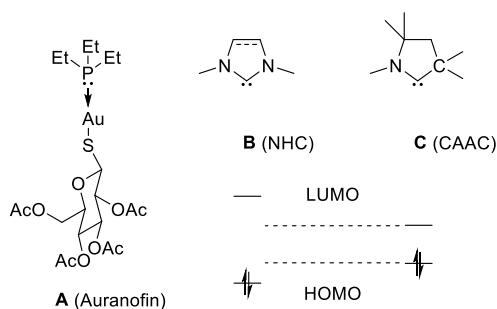
Supporting information for this article is given via a link at the end of the document. ((Please delete this text if not appropriate))

**Abstract:** Cyclic (Alkyl)(Amino)Carbenes (CAACs) have become forceful ligands for gold due to their ability to form very strong ligand-metal bonds. Inspired by the success of Auranofin and other gold complexes as antitumor agents, we have studied the cytotoxicity of bis- and mono-CAAC-gold complexes on different cancer cell lines: HeLa (cervical cancer), A549 (lung cancer), HT1080 (fibrosarcoma) and Caov-3 (ovarian cancer). Further investigations aimed at elucidating their mechanism of action are described. This includes quantification of affinities for TrxR, evaluation of their bioavailability and determination of associated cell death process. Moreover, Transmission Electron Microscopy (TEM) was used to study morphological changes upon exposure. Noticeably, a significant reduction in non-specific binding to serum proteins was observed with CAAC complexes when compared to Auranofin. These results confirm the potential of CAAC-gold complexes in biological environments, which may result in more specific drug-target interactions and decreased side effects.

## Introduction

Many civilizations, starting with ancient China, employed gold containing concoctions, long touted for their healing powers in the fight against disease.<sup>1</sup> In the late 19th century, scientific study began with the examination of gold(I) complexes against pulmonary tuberculosis,<sup>2</sup> and then later against rheumatoid arthritis.<sup>3</sup> The latter became a successful endeavor with a clear demonstration of the beneficial effect of gold-thiolate drugs. Introduced in the late 1970's, Auranofin (Scheme 1, **A**) proved very promising and was approved for clinical use in 1985.<sup>3a</sup> The antitumor activity of Auranofin was reported for the first time in 1979.<sup>4</sup> Since that time, numerous gold(I) complexes supported by phosphorous-, nitrogen- or carbon-based ligands have been investigated.<sup>5</sup> Although it is still not fully understood, the proposed mechanism is associated with the ability of Auranofin and other gold-based drugs to bind a selenocysteine moiety

located in the C-terminal active site of the Thioredoxin Reductase (TrxR) enzyme,<sup>6</sup> which is involved in controlling Reactive Oxygen Species (ROS) homeostasis.<sup>7</sup> It should be noted that the 2',3',4',6'-tetra-O-acetyl- $\beta$ -D-glucopyranosyl-1'-thiolate (Glc) moiety was selected due to the over-expression of the corresponding glucose transporters on cancerous cells, resulting in a higher uptake of the gold complex compared to versions lacking this anionic carbohydrate ligand.<sup>8</sup> Despite its potency, Auranofin suffers from significant side effects due to its undesired binding to cysteine residues on serum proteins and intracellular proteins.<sup>9</sup> A step forward in the design of gold(I) drugs was achieved with the replacement of the phosphine ligand by N-Heterocyclic Carbenes (NHCs) **B**,<sup>10,11</sup> which form stronger ligand-metal bonds. Similarly to Auranofin, neutral complexes of type Au(**B**)Cl mainly exhibit cytotoxicity to their ability to inhibit TrxR overexpressed in cancer cells. Alternatively, cationic bis-carbene complexes of type Au(**B**)<sup>2+</sup>X<sup>-</sup> show higher stability under physiological conditions than neutral complexes and are characterized by a better ability to navigate through membrane with elevated potential, to accumulate in the mitochondria, to interact with membranous vital systems and also to induce deregulation and/or alterations of elements essential for cell life.<sup>5d-f</sup>

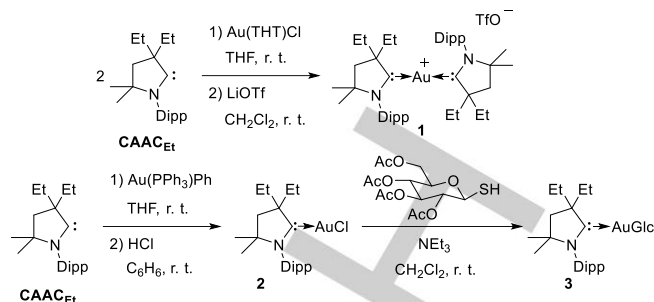


**Scheme 1.** Auranofin structure (**A**); frontier orbitals comparison between NHCs (**B**) and CAACs (**C**).

More recently, another family of carbenes, namely cyclic (alkyl)(amino) carbenes (CAACs)<sup>12,13</sup> **C** have found many applications, due to their peculiar steric and electronic properties. In-deed, when compared to NHCs, the replacement of one nitrogen atom ( $\sigma$ -attractor and  $\pi$ -donor) by a quaternary carbon (solely  $\sigma$ -donor) results in a higher HOMO (carbene lone pair) and lower LUMO (formal empty orbital) (Scheme 1).<sup>14</sup> Therefore, CAACs are simultaneously amongst the most basic and the most  $\pi$ -acidic singlet carbenes. The advantages of this class of carbene over NHCs are best exemplified by success in the isolation of active catalytic intermediates,<sup>15</sup> efficient and robust pre-catalysts,<sup>16</sup> and complexes with unusual configuration and/or oxidation states.<sup>17</sup> In all cases the stronger carbene-metal bond is characteristic of these CAAC bound complexes with respect to NHC analogs. There-fore, there is reason to believe that CAAC-bound gold complexes would exhibit lower affinity for cellular proteins compared to desired biological targets, leading to more specific drug-target interactions and decreased side effects. Recently, different CAAC-bound gold, silver and copper complexes have been reported as potent cytotoxic agents. Further, their mechanism of action appears to be metal dependent.<sup>18</sup> Herein, we report a detailed investigation on the in vitro antitumoral activity of a set of gold(I) complexes (*vide infra*) all bearing CAAC ancillary ligands for better comparison between them, namely  $[\text{Au}(\text{CAAC}_{\text{Et}})_2]^+\text{TfO}^-$  **1**,  $\text{Au}(\text{CAAC}_{\text{Et}})\text{Cl}$  **2**<sup>17d</sup> and  $\text{Au}(\text{CAAC}_{\text{Et}})\text{Glc}$  **3**. We have also evaluated the ability of these complexes to inhibit TrxR, measured their affinity for bovine serum albumin (BSA) and provide evidence for the mechanism of cell death.

## Results and Discussion

First, we reacted free carbene **CAAC**<sub>Et</sub> with a half-equivalent of Au(THT)Cl in tetrahydrofuran. Subsequent anion exchange by treating the cationic complex with lithium trifluoromethanesulfonate in methylene chloride afforded the homoleptic salt **1** in 91% yield (Scheme 2, top). The neutral complex **2** is prepared by a two-step sequence in which **CAAC**<sub>Et</sub> is first reacted with Au(PPh<sub>3</sub>)Ph to substitute the PPh<sub>3</sub> ligand. Then protolysis of the resulting Au(**CAAC**<sub>Et</sub>)Ph with dry HCl in benzene allowed for the isolation of the desired complex **2** in an overall yield of 87% (Scheme 2 bottom center). Note that both compounds **1** and **2** can be synthesized by bypassing the isolation of free carbene **CAAC**<sub>Et</sub>. In the former case, addition of one equivalent of KHMDS to the mixture of the cyclic iminium **CAAC**<sub>Et</sub>H<sup>+</sup>TfO<sup>-</sup> and Au(THT)Cl also led to complex **1**, albeit with overall lower yields of 62%. Similarly, addition of one equivalent of KHMDS to the mixture of the cyclic iminium **CAAC**<sub>Et</sub>H<sup>+</sup>TfO<sup>-</sup> and Au(PPh<sub>3</sub>)Ph and further reaction with HCl afforded complex **2** with an 82% yield. Finally, reaction of complex **2** with the gluco-pyranosyl-1-thiole in the presence of triethylamine in methylene chloride led to the expected CAAC-bound Auranofin analog **3** in good yield (94%, Scheme 2, bottom right). Each of these complexes were found to be indefinitely air and moisture stable, and were fully characterized by NMR, HR-MS and X-ray diffraction of single crystals (Figure 1).



**Scheme 2.** Syntheses of complexes **1** (top), **2** (bottom center) and **3** (bottom right).

As for any CAAC supported divalent gold(I) complex,<sup>19</sup> we expected a linear geometry at the metal center. Analysis of the solid-state structures<sup>20</sup> confirmed this spatial arrangement with C-Au-C/X angles of 170.56° (**1**), 178.05° (**2**) and 176.47° (**3**), respectively. The slightly bent geometry in the homoleptic complex **1** is unexpected with regards to previously reported  $[\text{Au}(\text{CAAC})_2]^+$  fragments in which the carbene-Au-carbene angle is found to be 180°. However, this bent geometry is commonly observed in bis-CAAC complexes of Ni(0),<sup>21a</sup> Pd(0)<sup>21b</sup> and Pt(0),<sup>21b</sup> which are isolobal to Au(I), and exhibit carbene-metal-carbene angles of 169° ± 4°. More importantly, in complex **1**, the trifluoromethanesulfonate anion is located more than 5 Å away from the gold atom and therefore does not engage in any interaction with the metal center. Finally, carbene-gold bond lengths remain relatively constant (**1**: 2.036 (3) Å, **2**: 1.975 (3) Å, **3**: 2.004 (4) Å). Note that the minor shortening of the carbene bond length for the gold-chloride complex has already been observed for analogous compounds.<sup>19</sup>

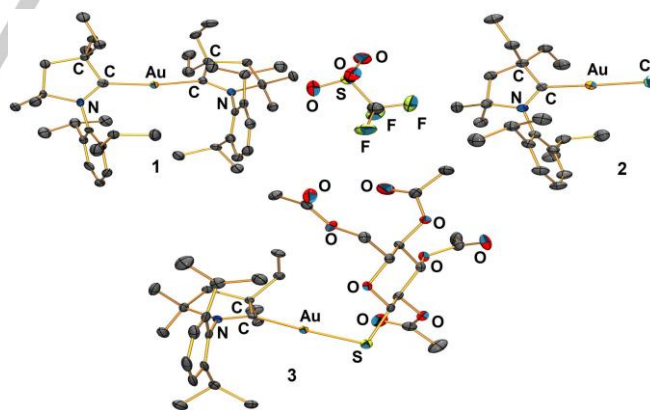


**Figure 1.** Solid-state structures of complexes **1**, **2** and **3**. Ortep views are shown with ellipsoids at 50% probability. H atoms, solvents are omitted for clarity.

With complexes **1-3** and the **CAAC**<sub>Et</sub>H<sup>+</sup>TfO<sup>-</sup> salt in hand, we tested their cytotoxicity against three different human cancer cell lines: HeLa (cervical cancer), A549 (lung cancer), HT1080 (fibrosarcoma) and Caov-3 (ovarian cancer). A cell titer blue assay was used to determine the extent of the inhibitory effect of the complexes on cancer cell growth. Cytotoxic activities were

demonstrated to be compound and cell line dependent: against HeLa cells, activities decreased following the order  $1 > 2 > 3 > \text{CAAC}_{\text{Et}}\text{H}^+\text{TfO}^-$ , whereas, against A549 and HT1080, the order  $1 > 3 > 2 > \text{CAAC}_{\text{Et}}\text{H}^+\text{TfO}^-$  was observed. Finally, the activities followed  $1 > 3 > 2 > \text{CAAC}_{\text{Et}}\text{H}^+\text{TfO}^-$  when exposed to Caov-3. Overall, Auranofin **A**,  $\text{Au}(\text{CAAC}_{\text{Et}})\text{Cl}$  **2** and  $\text{Au}(\text{CAAC}_{\text{Et}})\text{Glc}$  **3** triggered death on all cell lines with IC50 values in the micromolar range (Table 1). Interestingly,  $[\text{Au}(\text{CAAC}_{\text{Et}})_2]^+\text{TfO}^-$  **1** proved to be more cytotoxic than the others, with IC50 values lower by 1 to 2 orders of magnitude across all cell lines.

**Table 1.** Cytotoxicity (IC50) against cancer cell lines (in  $\mu\text{M}$ )<sup>[a]</sup>

| Compound  | HeLa      | A549        | HT1080      | Caov-3    |
|---|-----------|-------------|-------------|-----------|
| Auranofin <b>A</b>  | 1.7 ± 0.2 | 3.7 ± 0.6   | 1.4 ± 0.9   | 0.9 ± 0.3 |
| $[\text{Au}(\text{CAAC}_{\text{Et}})_2]^+\text{OTf}^-$ <b>1</b> | 0.3 ± 0.2 | 0.07 ± 0.06 | 0.14 ± 0.04 | 0.3 ± 0.2 |
| $\text{Au}(\text{CAAC}_{\text{Et}})\text{Cl}$ <b>2</b>          | 0.6 ± 0.2 | 4.5 ± 0.7   | 4.4 ± 1.3   | 3.9 ± 0.8 |
| $\text{Au}(\text{CAAC}_{\text{Et}})\text{Glc}$ <b>3</b>         | 2.7 ± 0.1 | 6.6 ± 2.5   | 3.1 ± 1.8   | 1.9 ± 0.4 |
| $\text{CAAC}_{\text{Et}}\text{H}^+\text{TfO}^-$                 | 60 ± 13   | 76 ± 34     | 26 ± 16     | > 50      |

[a] IC50 values represent the concentration that caused 50% cell death reported. These values were estimated by interpolation in the sigmoidal dose response fitted curve and are the results of at least three independent experiments

This trend has previously been observed for NHC supported gold(I) complexes and is linked to the ability of delocalized lipophilic cations to pass through hydrophobic barriers and mitochondrial membranes to reach their targets in the mitochondria.<sup>22</sup> Auranofin (**A**) was observed to be slightly more active than the  $\text{CAAC}_{\text{Et}}$ -analog **3** ( $\text{Au}(\text{CAAC}_{\text{Et}})\text{Glc}$ ) in all cell lines. Remarkably, compound **2** exhibited higher cytotoxicity than Auranofin only on HeLa cells, suggesting a cell dependent mechanism of action. Furthermore, the ligand precursor  $\text{CAAC}_{\text{Et}}\text{H}^+\text{OTf}^-$  was found to be at least 5- to 1000-fold less toxic than the complexes against this set of cancer cell lines. The significantly lower cytotoxicity of  $\text{CAAC}_{\text{Et}}\text{H}^+\text{OTf}^-$ , clearly demonstrates the gold center involvement in the antitumor activity. In general, the gold complexes bearing  $\text{CAAC}_{\text{Et}}$  as a mono- or bis- carrier ligand were demonstrably more active than those reported with bulkier CAAC-ligands,<sup>18</sup> suggesting that steric parameters and the hydrophilicity/lipophilicity balance are key features impacting activity.

Thus, as part of an investigation on the physicochemical properties of the CAAC-gold complexes, we determined their lipophilicity using the octanol-water partition protocol. Based on our experimental results, the most lipophilic compound was  $\text{Au}(\text{CAAC}_{\text{Et}})\text{Cl}$  **2**, followed by  $\text{Au}(\text{CAAC}_{\text{Et}})\text{Glc}$  **3**. As expected because of its positively charged nature  $[\text{Au}(\text{CAAC}_{\text{Et}})_2]^+\text{TfO}^-$  **1** showed the lowest lipophilicity value (Table 2). Indeed, it has been reported that the lipophilicity of compounds can be finely tuned to increase their ability to cross cellular membranes and accumulate in mitochondria, therefore modifying their toxicity.<sup>6,23</sup> To examine the impact of lipophilicity on cytotoxicity, we studied the cellular uptake of  $[\text{Au}(\text{CAAC}_{\text{Et}})_2]^+\text{TfO}^-$  **1**,  $\text{Au}(\text{CAAC}_{\text{Et}})\text{Cl}$  **2** and  $\text{Au}(\text{CAAC}_{\text{Et}})\text{Glc}$  **3** in Caov-3 at 1  $\mu\text{M}$  concentration after 6 h incubation. Our results showed a 10-fold greater uptake for the

cationic complex  $[\text{Au}(\text{CAAC}_{\text{Et}})_2]^+\text{TfO}^-$  **1** when compared to the neutral complexes  $\text{Au}(\text{CAAC}_{\text{Et}})\text{Cl}$  **2** and  $\text{Au}(\text{CAAC}_{\text{Et}})\text{Glc}$  **3**. Interestingly, complex  $\text{Au}(\text{CAAC}_{\text{Et}})\text{Cl}$  **2**, which is the most lipophilic compound, showed the lowest uptake and cytotoxicity values on Caov-3 cells. Among these CAAC-complexes, lower lipophilicity is associated with higher cellular uptake and higher cytotoxicity.

Based on the accepted mode of action for Auranofin **A** and other gold complexes, we opted to explore affinity towards TrxR, a known target for gold complexes. In parallel, we investigated non-specific interactions between gold complexes and serum proteins, using bovine serum albumin as a model. Compounds **A**, **1**, **2** and **3** were incubated with TrxR and bovine serum albumin and results are summarized in Table 2.

**Table 2.** LogP values, Cellular Uptake, TrxR Inhibition and % BSA binding

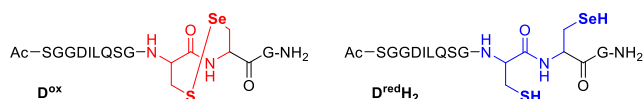
| Compound  | LogP      | Uptake (ng Au/mg protein) <sup>[a]</sup> | TrxR (IC50, nM) <sup>[b]</sup> | BSA binding (%) <sup>[c]</sup> |
|---|-----------|--|--------------------------------|--------------------------------|
| Auranofin <b>A</b>  | n.d.[d]   | n.d.[d]                                  | 15.6 ± 4.7                     | 79 ± 6                         |
| $[\text{Au}(\text{CAAC}_{\text{Et}})_2]^+\text{OTf}^-$ <b>1</b> | 1.4 ± 0.1 | 276 ± 115                                | >100,000                       | 17 ± 21 [c]                    |
| $\text{Au}(\text{CAAC}_{\text{Et}})\text{Cl}$ <b>2</b>          | 2.4 ± 0.1 | 28 ± 11                                  | 819 ± 145                      | 55 ± 9                         |
| $\text{Au}(\text{CAAC}_{\text{Et}})\text{Glc}$ <b>3</b>         | 2.2 ± 0.2 | 36 ± 8                                   | 2,226 ± 826                    | 50 ± 9                         |
| $\text{CAAC}_{\text{Et}}\text{H}^+\text{TfO}^-$                 | n.d.[d]   | n.d.[d]                                  | >200,000                       | n.d.[d]                        |

[a] Uptake in Caov-3 cells after 6 h incubation with 1  $\mu\text{M}$  of the respective Au-complex. [b] IC50 values represent the concentration that caused 50% cell death reported. [c] BSA binding was estimated as the percentage of free drug recovered in the presence and absence of protein. [d] not determined

Under our protocol and in accordance with previously published literature,<sup>24</sup> Auranofin **A** showed the highest TrxR inhibitory effect at low nanomolar concentrations. Complex **2** showed increased activity over **3**, with both exhibiting TrxR-IC50 values in the micromolar ranges. Note that previously reported, analogous NHC and CAAC complexes show TrxR inhibition at similar concentration ranges.<sup>25</sup> Interestingly, despite displaying the highest cytotoxicity against all cancer cell lines studied here, the cationic complex  $[\text{Au}(\text{CAAC}_{\text{Et}})_2]^+\text{TfO}^-$  **1** did not inhibit TrxR up to its solubility limit (100  $\mu\text{M}$ ). Moreover, as expected,  $\text{CAAC}_{\text{Et}}\text{H}^+\text{TfO}^-$  bearing no gold metal center, was demonstrated to have no affinity for TrxR up to its solubility limit.

To further understand TrxR inhibition by the gold complexes, we chose to study the binding of gold complexes **1-3** with dodecapeptide  $\text{D}^{\text{ox}}$  (Ac-SGGDILQSGCUG-NH<sub>2</sub>, Scheme 3)<sup>6b</sup> which is analogous to the peptide sequence found in TrxR that is the specific target of gold complexes. Note that in its oxidized form,  $\text{D}^{\text{ox}}$  corresponds to the non-active form of the TrxR enzyme. Peptide  $\text{D}^{\text{ox}}$  was prepared according to literature procedures and was converted into  $\text{D}^{\text{redH}_2}$  (Ac-SGGDILQSGC<sub>H</sub>U<sub>H</sub>G-NH) upon treatment with tris(2-carboxyethyl)phosphine (TCEP). Under its reduced form,  $\text{D}^{\text{redH}_2}$ , as well as analogous deprotonated forms of the reduced peptide ( $\text{D}^{\text{redH}}$  and  $\text{D}^{\text{red}2-}$ ), correspond to the active forms of the TrxR. To investigate the interactions between the gold complexes and peptides of type **D**, we incubated freshly reduced peptide  $\text{D}^{\text{redH}_2}/\text{D}^{\text{redH}}/\text{D}^{\text{red}2-}$  with gold complexes **1-3** and analyzed the

results by mass spectrometry. As expected, complexes **2** and **3** form anionic adducts  $[\mathbf{D}^{\text{red}}\text{-Au}(\text{CAAC}_{\text{Et}})]$  in which the reduced dianionic peptide  $\mathbf{D}^{\text{red},2-}$  is bound to the  $[\text{CAAC-Au}]^+$  cationic fragment resulting from the formal substitution of the anionic ligand (X= Cl<sup>-</sup> for **2** or X= Glc<sup>-</sup> for **3**).



**Scheme 3.** Dodecapeptide **D**, analogous to TrxR active sequence, in its oxidized ( $\mathbf{D}^{\text{ox}}$ ) and reduced ( $\mathbf{D}^{\text{redH}_2}$ ) forms.

Interestingly, incubation of the cationic complex **1** under the same conditions as above, did not allow for observation of the corresponding adduct  $[\mathbf{B}^{\text{red}}\text{-Au}(\text{CAAC}_{\text{Et}})_2]$ ; thus, explaining the lack of inhibition of TrxR detailed in Table 2.

As stated, one of our goals was to overcome concerns regarding the undesired affinity of Auranofin to albumin. Here, all complexes showed reduced binding compared to Auranofin **A** (See Table 2). Moreover, compared to similar NHC supported gold complexes,<sup>26</sup> the use of CAAC ligands lead to decreased non-specific binding from close to 100%<sup>27</sup> to 55%. We believe the lower affinity of CAAC-supported complexes **1**, **2** and **3** to BSA compared to **A** and NHC analogs complexes is a result of the stronger ligand-metal bond, and thus the greater stability of complexes **1**, **2** and **3**.

Several important pieces of information arise from these data. First, it appears that the cytotoxicity of complex **1** results without targeting the TrxR enzyme, hence causing cell death through a mechanism different than for complexes **A**, **2** and **3**. Also, even though the lack of interaction between  $[\text{Au}(\text{CAAC}_{\text{Et}})_2]^+\text{TfO}^-$  **1** and the selenocysteine moiety is not surprising, it does suggest that the CAAC ligand is not labile under these conditions, and that the fragment  $[\text{Au}(\text{CAAC}_{\text{Et}})_2]^+$  retains its structural integrity. Again, this stability is a clearly the result of the stronger carbene-metal bond strength compared to other supporting ligands.<sup>28</sup> Finally, while the Auranofin **A** inhibition of TrxR, in the nanomolar range, is much stronger than complexes **2** and **3**, the higher propensity of **A** to undergo non-selective binding to BSA<sup>29</sup> partially accounts for similar cytotoxicity observed for complexes **A**, **2** and **3**. Indeed, in contrast to **A**, complexes **2** and **3** inhibit TrxR in the micromolar range but show lower non-specific binding. In other words, taken together, the results from Table 1 and 2 confirm the high efficiency at which CAAC-bound complexes reach their biological target and may be reflected less by lower affinity, non-specific interactions with other, undesired, biomolecular targets. This increased selectivity might also result in improved bioavailability and bio-distribution profiles which are important parameters for experimental drugs at the developmental stage.

After establishing these intrinsic features, we decided to investigate the modes of cell death (necrosis vs. apoptosis) induced by each compound, **A**, **1**, **2** and **3**. We used a standard protocol in which HeLa cells were incubated with our set of gold compounds (10  $\mu\text{M}$ ) and their effects were studied in a time-dependent manner. Thus, at each selected time-point, cells were stained with FITC-Annexin V and Propidium Iodide (PI). Annexin V is a protein that binds to phosphatidylserine, a lipid constituent of plasma membrane which is normally restricted to

the inner membrane surface but becomes exposed in the outer leaflet when cells undergo apoptosis. PI is used as a marker of cell membrane integrity and combined with Annexin V it becomes a tool to distinguish necrotic from apoptotic cells using flow cytometry.<sup>30</sup>

Analysis at various selected times, show that complexes **A**, **2** and **3** induce apoptosis at early time-points, after which cells probably undergo secondary necrosis resulting in an increase of necrotic cells with respect to cells undergoing apoptosis. Among this series of compounds, the glucopyranosyl containing complex **3** stands out as the most potent cell death promoter, with almost 80% of the total population of cells undergoing either apoptosis or necro-sis. Interestingly, when exposed to  $[\text{Au}(\text{CAAC}_{\text{Et}})_2]^+\text{TfO}^-$  **1** for a duration of up to 6 h, a negligible amount of cells undergo either apoptosis or necrosis. These results, as well as the previously discussed lack of TrxR inhibition exhibited by  $[\text{Au}(\text{CAAC}_{\text{Et}})_2]^+\text{TfO}^-$  **1**, supports the hypothesis that its cell death mechanism involves a different pathway than the gold complexes bearing only one CAAC ligand.

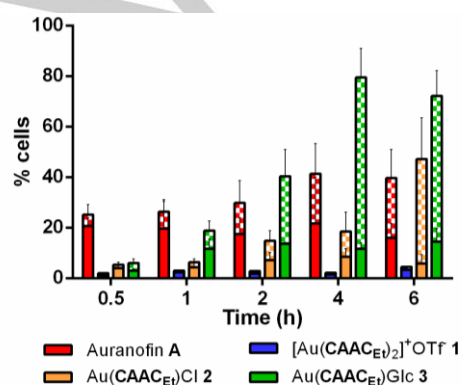


**Figure 2.** Population of apoptotic vs. necrotic HeLa cells after a 30 min to 6 h exposure to complexes **A**, **1**, **2** and **3**. Full bars represent % cells undergoing apoptosis, while gridded bars represent cells under-going necrosis. The height of the bars represents the % of cells undergoing apoptosis and necrosis.

To further understand these results, we studied the ability of these compounds to induce depolarization and loss of mitochondrial trans-membrane potential ( $\Delta\Psi\text{m}$ ), which is closely related to apoptotic cellular pathways.<sup>31</sup> To test this, we employed a lipophilic cationic dye, 5,5',6,6'-tetrachloro-1,1',3,3'-tetraethylbenzimidazolylcarbocya-nine iodide (JC-1), which is known to enter mitochondria and arrange in red fluorescent J-aggregates on cells with high  $\Delta\Psi\text{m}$ . Upon mitochondrial membrane depolarization JC-1 remains in its green fluorescent monomeric form. Flow cytometry plots were obtained (FL1, green vs. FL2, red) for HeLa cells pretreated with Auranofin **A**,  $[\text{Au}(\text{CAAC}_{\text{Et}})_2]^+\text{TfO}^-$  **1**,  $\text{Au}(\text{CAAC}_{\text{Et}})\text{Cl}$  **2**,  $\text{Au}(\text{CAAC}_{\text{Et}})\text{Glc}$  **3** or dimethylformamide (DMF, solvent control) and subsequently stained with JC-1 (Figure S7). A healthy cell population was gated on an untreated cell sample (P1, double positive) and compared to the plot from the cells incubated with DMF or the gold complexes. Accordingly, a significant decrease of red fluorescent aggregates in cells exposed to Auranofin **A**,  $\text{Au}(\text{CAAC}_{\text{Et}})\text{Cl}$  **2** and  $\text{Au}(\text{CAAC}_{\text{Et}})\text{Glc}$  **3** can be observed. Once more, the latter display the largest effect, while  $[\text{Au}(\text{CAAC}_{\text{Et}})_2]^+\text{TfO}^-$  **1**, showed only minimal decrease on J-aggregates or mitochondrial depolarization, suggesting a different mechanism of action.

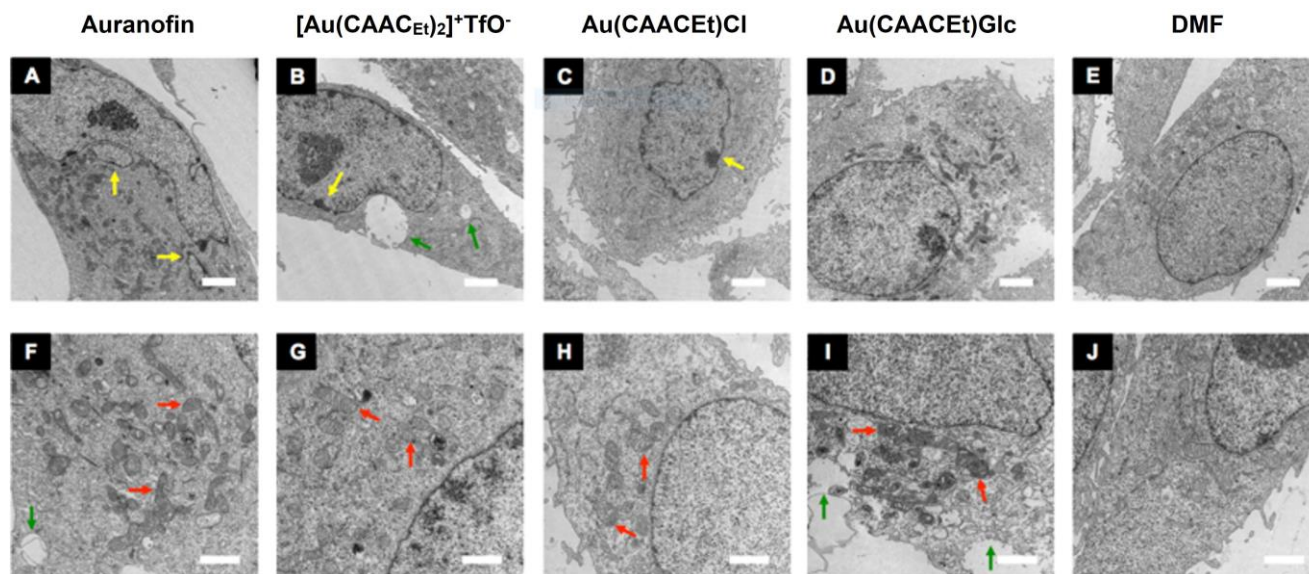


**Figure 3.** TEM images of cells pretreated with Auranofin A (A, F),  $[\text{Au}(\text{CAAC}_{\text{Et}})_2]^+\text{TfO}^-$  **1** (B, G),  $\text{Au}(\text{CAAC}_{\text{Et}})\text{Cl}$  **2** (C, H),  $\text{Au}(\text{CAAC}_{\text{Et}})\text{Glc}$  **3** (D, I) at a 10  $\mu\text{M}$  concentration and DMF as a vehicle control (E, J). Top panels show low magnification images (x2,900, A-E, scale bars represent 2  $\mu\text{m}$ ) and bottom panels show high magnification images (x6,800, F-J, scale bars represent 1  $\mu\text{m}$ ). Specific features of cell morphologies are shown with arrows (further discussion in the main text).

Apoptosis and necrosis are the result of different biochemical events, which can be monitored as cellular morphological changes.<sup>32</sup> Owing to its high resolution and the possibility of introducing high-contrast staining agents to the samples, Transmission Electron Microscopy (TEM) is widely used to study cellular ultra-structures. Therefore, HeLa cells were incubated with DMF solutions of complexes Auranofin **A**,  $[\text{Au}(\text{CAAC}_{\text{Et}})_2]^+\text{TfO}^-$  **1**,  $\text{Au}(\text{CAAC}_{\text{Et}})\text{Cl}$  **2** and  $\text{Au}(\text{CAAC}_{\text{Et}})\text{Glc}$  **3** (10  $\mu\text{M}$ ) plus a control voided of any gold complex for 30 min and processed for TEM imaging. Representative TEM micrographs of cells exposed to gold complexes are shown in low magnification (x2,900, Figure 3A-D) and high magnification (x6,800, Figure 3F-I). Lastly, TEM micro-graphs of the control experiment, with cells exposed to only DMF (Figure 3E and 3J) were obtained to ascertain the effect of each gold complex.

We consider normal cellular morphologies as rounded with homogenous cellular and nuclear membranes, each containing a nucleolus, chromatin, in addition to well-preserved cytoplasmic organelles. Auranofin **A** (Figure 3A and 3F) is well known to promote apoptosis on a wide variety of cancer cells.<sup>33</sup> Under our experimental protocol, we could observe clear signs of apoptosis such as nuclear fragmentation or karyorrhexis (Figure 3A, yellow arrows), and swollen cytoplasmic organelles and vacuoles (Figure 3F, red and green arrows respectively).<sup>32b,34</sup>  $\text{Au}(\text{CAAC}_{\text{Et}})\text{Cl}$  **2** (Figure 3C and 3H) pretreated cells show morphological signs of early apoptosis such as condensation of chromatin at the nuclear membrane (Figure 3C, yellow arrow) and preserved mitochondria (Figure 3H, red arrows). Cells exposed to  $\text{Au}(\text{CAAC}_{\text{Et}})\text{Glc}$  **3** (Figure 3D and 3I) show the highest degree of pathological morphological features with cells transitioning from apoptosis to secondary necrosis such as swelling of mitochondria and disruption of plasma membrane (Figure 3I, red and green arrows respectively). In contrast, cells exposed to  $[\text{Au}(\text{CAAC}_{\text{Et}})_2]^+\text{TfO}^-$  **1**, (Figure 3B and 3G) show well rounded nuclei and preserved cytoplasmic organelles (Figure

3G, red arrows). Some degree of chromatin fragmentation and cytoplasmic vacuoles were observed (Figure 3B, yellow and green arrows respectively), which may suggest a population of cells undergoing early apoptosis.

## Conclusion

In conclusion, we have demonstrated the effect of a CAAC ligand as a gold ligand in anticancer cell studies. As previously reported with NHC supported complexes, mono- and bis-CAAC gold com-plexes possess different cellular targets.<sup>7b</sup> Both mono- and bis-CAAC supported gold centers benefit from the peculiar coordination environment and intrinsic electronic properties provided by the CAAC ligand. As a result, this new family of cytotoxic agents demonstrated significantly reduced non-specific binding toward non-tumor associated proteins such as albumin, while still retaining high affinity to the target TrxR ( $\text{Au}(\text{CAAC}_{\text{Et}})\text{Cl}$  **2** and  $\text{Au}(\text{CAAC}_{\text{Et}})\text{Glc}$  **3**). Moreover, morphological and biochemical changes suggest that  $\text{Au}(\text{CAAC}_{\text{Et}})\text{X}$  complexes **2** and **3** induce cell death through a mechanism indicative of apoptosis followed by secondary necrosis.  $[\text{Au}(\text{CAAC}_{\text{Et}})_2]^+\text{TfO}^-$  **1**, showed the highest cytotoxic activity with an onset of activity at longer time-points than the mono-ligated complexes and no affinity to TrxR. Therefore, other mechanisms of action need to be considered, such as the induction of Mitochondrial Membrane Permeabilization,<sup>35</sup> or binding to telomeric DNA G-quadruplexes.<sup>36</sup> Such mechanisms of action unrelated to TrxR inhibition are currently under investigation for  $[\text{Au}(\text{CAAC}_{\text{Et}})_2]^+\text{TfO}^-$  **1**. Altogether this investigation reports on the applicability of CAAC-supported gold complexes with application as antitumor agents and reveals their biological targets which may lead to lower undesired side-effects for gold metal-based therapeutics.

## Acknowledgements

Thanks are due to the US National Science Foundation (CHE-1954380). M. T. P. thanks the UCSD Cancer Researchers in Nanotechnology (CRIN) for a postdoctoral fellowship and the mentorship of Dr A. Kummel within that program.

**Keywords:** Antitumoral Agents • CAACs • Cancer • Transmission Electron Microscopy • TrxR

- [1] H. Zhao, Y. Ning, *Gold Bull.* **2001**, *34*, 24-29.
- [2] R. Koch, *Dtsch. Med. Wochenstr.* **1890**, *16*, 756-757.
- [3] (a) W. F. Kean, F. Forestier, Y. Kassam, W. W. Buchanan, A. G. Rooney, *Semin. Arthritis Rheum.* **1985**, *14*, 180-186. (b) W. F. Kean, C. J. L. Lock, H. Howard-Lock, *Inflammopharmacology* **1991**, *1*, 103-114. (c) W. F. Kean, L. Hart, W. W. Buchanan, *Rheumatology* **1997**, *36*, 560-572; (d) A. G. Baldwin, D. Brough, S. Freeman, *J. Med. Chem.* **2016**, *59*, 1691-1710.
- [4] T. M. Simon, D. H. Kunishima, G. J. Vibert, A. Lorber, *Cancer* **1979**, *44*, 1965-1975.
- [5] (a) S. J. Berners-Price, A. Filipovska, *Metallomics* **2011**, *3*, 863-873. (b) C. Schmidt, L. Albrecht, R. M. Balasupramaniam, B. Karge, M. Brönstrup, A. Prokop, K. Baumann, S. Reichl, I. Ott, *Metallomics* **2019**, *11*, 533-545. (c) J. L. Hickey, R. A. Ruhayel, P. J. Barnard, M. V. Baker, S. J. Berners-Price, A. Filipovska, *J. Am. Chem. Soc.* **2008**, *130*, 12570-12571. (d) W. Liu, R. Gust, *Coord. Chem. Rev.* **2016**, *329*, 191-213. (e) M. Mora, M. C. Gimeno, R. Visbal, *Chem. Soc. Rev.* **2019**, *48*, 447-462. (f) C. H. G. Jakob, Bruno Dominelli, E. M. Hahn, T. O. Berghausen, T. Pinheiro, F. Marques, R. M. Reich, J. D. G. Correia, F. E. Kühn, *Chem Asian J.* **2020**, *15*, 2754-2762. (g) F. Magherini, T. Fiaschi, E. Valocchia, M. Becatti, A. Pratesi, T. Marzo, L. Massai, C. Gabbiani, I. Landini, S. Nobili, E. Mini, L. Messori, A. Modesti, T. Gamberi, *Oncotarget*, **2018**, *9*, 28042-28068
- [6] (a) F. Angelucci, A. A. Sayed, D. L. Williams, G. Boumis, M. Brunori, D. Dimastrogiovanni, A. E. Miele, F. Pauly, A. Bellelli, *J. Biol. Chem.* **2009**, *284*, 28977-28985. (b) A. Pratesi, C. Gabbiani, E. Michelucci, M. Ginanneschi, A. M. Papini, R. Rubbiani, I. Ott, L. Messori, *J. Inorg. Biochem.* **2014**, *136*, 161-169.
- [7] (a) D. Trachootham, J. Alexandre, P. Huang, *Nat Rev Drug Discov* **2009**, *8*, 579-591. (b) W. Liu, K. Bendsdorf, M. Proetto, A. Hagenbach, U. Abram, R. Gust, *J. Med. Chem.* **2012**, *55*, 3713-3724.
- [8] (a) D. A. Chan, P. D. Sutphin, P. Nguyen, S. Turcotte, E. W. Lai, A. Banh, G. E. Reynolds, J. -T. Chi, J. Wu, D. E. Solow-Cordero, *et al. Sci. Transl. Med.* **2011**, *3*, 94ra70. (b) A. K. Buck, S. N. Reske, *J. Nucl. Med.* **2004**, *45*, 461-463.
- [9] M. S. Iqbal, S. G. Taqi, M. Arif, M. Wasim, M. Sher, *Biol. Trace Elem. Res.* **2009**, *130*, 204-209.
- [10] For thematic issues and books on NHCs, see: (a) T. Rovis, S. P. Nolan, *Synlett* **2013**, *24*, 1188-1189. (b) A. J. Arduengo, G. Bertrand, *Chem. Rev.* **2009**, *109*, 3209-3210. (c) S. Díez-González, in *N-Heterocyclic Carbenes: From Laboratory Curiosities to Efficient Synthetic Tools*, Royal Society of Chemistry: Cambridge, **2016**. (d) Nolan, S. P. in *N-Heterocyclic Carbenes: Effective Tools for Organometallic Synthesis*; Wiley-VCH: Weinheim, **2014**.
- [11] (a) K. M. Hindi, M. J. Panzner, C. A. Tessier, C. L. Cannon, W. J. Youngs, *Chem. Rev.* **2009**, *109*, 3859-3884. (b) W. Liu, R. Gust, *Chem. Soc. Rev.* **2013**, *42*, 755-773.
- [12] For the synthesis of CAACs, see: (a) V. Lavallo, Y. Canac, C. Präsang, B. Donnadieu, G. Bertrand, *Angew. Chem.* **2005**, *117*, 5851-5855; *Angew. Chem., Int. Ed.* **2005**, *44*, 5705-5709. (b) V. Lavallo, Y. Canac, A. DeHope, B. Donnadieu, G. Bertrand, *Angew. Chem.* **2005**, *117*, 7402-7405; *Angew. Chem., Int. Ed.* **2005**, *44*, 7236-7239; (c) R. Jazar, R. D. Dewhurst, J. B. Bourg, B. Donnadieu, Y. Canac, G. Bertrand, *Angew. Chem.* **2007**, *119*, 2957-2960; *Angew. Chem., Int. Ed.* **2007**, *46*, 2899-2902. (d) X. Zeng, G. D. Frey, R. Kinjo, B. Donnadieu, G. Bertrand, *J. Am. Chem. Soc.* **2009**, *131*, 8690-8696. (e) J. Chu, D. Munz, R. Jazar, M. Melaimi, G. Bertrand, *J. Am. Chem. Soc.* **2016**, *138*, 7884-7887.
- [13] For reviews on CAACs see: (a) M. Soleilhavoup, G. Bertrand, *Acc. Chem. Res.* **2015**, *48*, 256-266. (b) M. Melaimi, M. Soleilhavoup, G. Bertrand, *Angew. Chem.* **2010**, *122*, 8992-9032; *Angew. Chem., Int. Ed.* **2010**, *49*, 8810-8849. (c) S. Roy, K. C. Mondal, H. W. Roesky, *Acc. Chem. Res.* **2016**, *49*, 357-369. (d) M. Melaimi, R. Jazar, M. Soleilhavoup, G. Bertrand, *Angew. Chem.* **2017**, *129*, 10180-10203; *Angew. Chem., Int. Ed.* **2017**, *56*, 10046-10068. (e) R. Jazar, M. Soleilhavoup, G. Bertrand, *Chem. Rev.* **2020**, *120*, 4141-4168.
- [14] (a) V. Lavallo, Y. Canac, B. Donnadieu, W. W. Schoeller, G. Bertrand, *Angew. Chem.* **2006**, *118*, 3568-3571; *Angew. Chem., Int. Ed.* **2006**, *45*, 3488-3491. (b) O. Back, M. Henry-Ellinger, C. D. Martin, D. Martin, G. Bertrand, *Angew. Chem.* **2013**, *125*, 3011-3015; *Angew. Chem., Int. Ed.* **2013**, *52*, 2939-2943.
- [15] (a) L. Jin, D. R. Tolentino, M. Melaimi, G. Bertrand, *Sci. Adv.* **2015**, *1*, e1500304. (b) L. Jin, E. A. Romero, M. Melaimi, G. Bertrand, *J. Am. Chem. Soc.* **2015**, *137*, 15696-15699. (c) R. Kinjo, B. Donnadieu, G. Bertrand, *Angew. Chem.* **2011**, *123*, 5674-5677; *Angew. Chem., Int. Ed.* **2011**, *50*, 5560-5563.
- [16] (a) V. Lavallo, G. D. Frey, S. Kousar, B. Donnadieu, G. Bertrand, *Proc. Natl. Acad. Sci. USA* **2007**, *104*, 13569-13573. (b) V. M. Marx, A. H. Sullivan, M. Melaimi, S. C. Virgil, B. K. Keitz, D. S. Weinberger, G. Bertrand, R. G. Grubbs, *Angew. Chem.* **2015**, *127*, 1939-1943; *Angew. Chem., Int. Ed.* **2015**, *54*, 1919-1923.
- [17] (a) D. S. Weinberger, M. Melaimi, C. E. Moore, A. L. Rheingold, G. Frenking, P. Jerabek, G. Bertrand, *Angew. Chem.* **2013**, *125*, 9134-9137; *Angew. Chem., Int. Ed.* **2013**, *52*, 8964-8967. (b) D. S. Weinberger, S. K. N. Amin, K. C. Mondal, M. Melaimi, G. Bertrand, A. C. Stückl, H. W. Roesky, B. Dittrich, S. Demeshko, B. Schwederski, W. Kaim, P. Jerabek, G. Frenking, *J. Am. Chem. Soc.* **2014**, *136*, 6235-6238. (c) L. Jin, D. S. Weinberger, M. Melaimi, C. E. Moore, A. L. Rheingold, G. Bertrand, *Angew. Chem.* **2014**, *126*, 9205-9209; *Angew. Chem., Int. Ed.* **2014**, *53*, 9059-9063. (d) L. Jin, M. Melaimi, A. Kostenko, M. Karni, Y. Apeloig, C. E. Moore, A. L. Rheingold, G. Bertrand, *Chem. Sci.* **2016**, *7*, 150-154.
- [18] B. Bertrand, A. S. Romanov, M. Brooks, J. Davis, C. Schmidt, I. Ott, M. O'Connell, M. Bochmann, *Dalton Trans.* **2017**, *46*, 15875-15887. (b) M. R. M. Williams, B. Bertrand, J. Fernandez-Cestau, Z. A. E. Waller, M. A. O'Connell, M. Searcey, M. Bochmann, *Dalton Trans.* **2018**, *47*, 13523-13534. (c) B. Bertrand, M. R. M. Williams, M. Bochmann, *Chem. Eur. J.* **2018**, *24*, 11840-11851.
- [19] G. D. Frey, R. D. Dewhurst, S. Kousar, B. Donnadieu, G. Bertrand, *J. Organomet. Chem.* **2008**, *693*, 1674-1682.
- [20] CCDC 2022581 ([Au(CAAC<sub>E1</sub>)<sub>2</sub>]<sup>+</sup>TfO<sup>-</sup> **1**), 2022582 (Au(CAAC<sub>E1</sub>)Cl **2**) and 2022583 (Au(CAAC<sub>E1</sub>)Glc **3**) contain the supplementary crystallographic data for this paper. These data can be obtained free of charge from the Cambridge Crystallographic Data Centre.
- [21] (a) K. C. Mondal, P. P. Samuel, Y. Li, H. W. Roesky, S. Roy, L. Ackermann, N. S. Sidhu, G. M. Sheldrick, E. Carl, S. Demeshko, S. De, P. Parameswaran, L. Ungur, L. F. Chibotaru, D. M. A. Andrada, *Eur. J. Inorg. Chem.* **2014**, 818-823. (b) S. Roy, K. C. Mondal, J. Meyer, B. Niepotter, C. Kohler, R. Herbst-Irmer, D. Stalke, B. Dittrich, D. M. Andrada, G. Frenking, H. W. Roesky, *Chem. Eur. J.* **2015**, *21*, 9312-9318.
- [22] (a) J. S. Modica-Napolitano, J. R. Aprile, *Adv. Drug Delivery Rev.* **2001**, *49*, 63-70; (b) S. J. Berners-Price, A. Filipovska, *Aust. J. Chem.* **2008**, *61*, 661-668.
- [23] (a) A. Bindoli, M. P. Rigobello, G. Scutari, C. Gabbiani, A. Casini, L. Messori, *Coord. Chem. Rev.* **2009**, *253*, 1692-1707. (c) R. Rubbiani, I. Kitanovic, H. Alborzinia, S. Can, A. Kitanovic, L. A. Onambele, M. Stefanopoulou, Y. Geldmacher, W. S. Sheldrick, G. Wolber, A. Prokop, S. Wölfl, I. Ott, *J. Med. Chem.* **2010**, *53*, 8608-8618.
- [24] W. Liu, K. Bendsdorf, M. Proetto, U. Abram, A. Hagenbach, R. Gust, *J. Med. Chem.* **2011**, *54*, 8605-8615.
- [25] W. Walther, O. Dada, C. O'Beirne, I. Ott, G. Sánchez-Sanz, C. Schmidt, C. Werner, X. Zhu, M. Tacke, *Lett. Drug Des. Discov.* **2017**, *14*, 125-134.

- [26] C. Schmidt, B. Karge, R. Misgeld, A. Prokop, M. Brönstrup, I. Ott, *Med. Chem. Commun.* **2017**, *8*, 1681-1689.
- [27] C. Schmidt, B. Karge, R. Misgeld, A. Prokop, R. Franke, M. Brönstrup, I. Ott, *Chem. Eur. J.* **2017**, *23*, 1869-1880.
- [28] (a) H. Sivaram, J. Tan, H. V. Huynh, *Organometallics* **2012**, *31*, 5875-5883. (b) H. F. Dos Santos, M. A. Viera, G. Y. Sánchez Delgado, D. Paschoal, *J. Phys. Chem. A* **2016**, *120*, 2250-2259.
- [29] Non-specific binding of Auranofin **A** to HSA, in the range of 60 to 80 %, is a well-studied phenomenon that results in higher required concentration to cause cell death: see reference 9
- [30] L. C. Crowley, B. J. Marfell, A. P. Scott, N. J. Waterhouse, *Cold Spring Harb. Protoc.* **2016**, *2016*, pdb prot087288.
- [31] J. D. Ly, D. R. Grubb, A. Lawen, *Apoptosis* **2003**, *8*, 115-128.
- [32] (a) J. F. Kerr, A. H. Wyllie, A. R. Currie, *Br. J. Cancer* **1972**, *26*, 239-257; (b) U. Ziegler, *News Physiol Sci* **2004**, *19*, 124-128.
- [33] (a) P. Zou, M. X. Chen, J. S. Ji, W. Q. Chen, X. Chen, S. L. Ying, J. R. Zhang, Z. H. Zhang, Z. G. Liu, S. L. Yang, G. Liang, *Oncotarget* **2015**, *6*, 36505-36521. (b) N. Park, Y. J. Chun, *J Toxicol Env Heal A* **2014**, *77*, 1467-1476.
- [34] (a) D. V. Krysko, T. Vanden Berghe, K. D'Herde, P. Vandenabeele, *Methods* **2008**, *44*, 205-221. (b) S. Elmore, *Toxicol Pathol* **2007**, *35*, 495-516.
- [35] M. V. Baker, P. J. Barnard, S. J. Berners-Price, S. K. Brayshaw, J. L. Hickey, B. W. Skelton, A. H. White, *Dalton Trans.* **2006**, 3708-3715.
- [36] C. Bazzicalupi, M. Ferraroni, F. Papi, L. Massai, B. Bertrand, L. Messori, P. Gratteri, A. Casini, *Angew. Chem.* **2016**, *128*, 4328-4331; *Angew. Chem. Int. Ed.* **2016**, *55*, 4256-4259.